



Neocerebellar Crus I Abnormalities Associated with a Speech and Language Disorder Due to a Mutation in *FOXP2*

G. P. D. Argyropoulos^{1,2} · K. E. Watkins³ · E. Belton-Pagnamenta^{1,4} · F. Liégeois¹ · K. S. Saleem⁵ · M. Mishkin⁵ · F. Vargha-Khadem^{1,6}

Published online: 20 November 2018
© The Author(s) 2018

Abstract

Bilateral volume reduction in the caudate nucleus has been established as a prominent brain abnormality associated with a *FOXP2* mutation in affected members of the ‘KE family’, who present with developmental orofacial and verbal dyspraxia in conjunction with pervasive language deficits. Despite the gene’s early and prominent expression in the cerebellum and the evidence for reciprocal cerebellum-basal ganglia connectivity, very little is known about cerebellar abnormalities in affected KE members. Using cerebellum-specific voxel-based morphometry (VBM) and volumetry, we provide converging evidence from subsets of affected KE members scanned at three time points for grey matter (GM) volume reduction bilaterally in neocerebellar lobule VIIa Crus I compared with unaffected members and unrelated controls. We also show that right Crus I volume correlates with left and total caudate nucleus volumes in affected KE members, and that right and total Crus I volumes predict the performance of affected members in non-word repetition and non-verbal orofacial praxis. Crus I also shows bilateral hypo-activation in functional MRI in the affected KE members relative to controls during non-word repetition. The association of Crus I with key aspects of the behavioural phenotype of this *FOXP2* point mutation is consistent with recent evidence of cerebellar involvement in complex motor sequencing. For the first time, specific cerebello-basal ganglia loops are implicated in the execution of complex oromotor sequences needed for human speech.

Keywords *FOXP2* · Verbal dyspraxia · Cerebellum · Caudate nucleus · MRI · VIIa crus I

Electronic supplementary material The online version of this article (<https://doi.org/10.1007/s12311-018-0989-3>) contains supplementary material, which is available to authorized users.

✉ F. Vargha-Khadem
f.vargha-khadem@ucl.ac.uk

¹ Cognitive Neuroscience and Neuropsychiatry Section, UCL Great Ormond Street Institute of Child Health, University College London, 30 Guilford Street, London WC1N 1EH, UK

² Nuffield Department of Clinical Neurosciences, University of Oxford, Oxford, UK

³ Department of Experimental Psychology, University of Oxford, Oxford, UK

⁴ School of Psychology and Clinical Language Sciences, University of Reading, Reading, UK

⁵ Laboratory of Neuropsychology, National Institute of Mental Health, Bethesda, MD, USA

⁶ Great Ormond Street Hospital for Children National Health Foundation Trust, London, UK

Introduction

A dominantly inherited constellation of speech and language deficits in half the members of the multi-generational ‘KE family’ [1–3] has been linked to a mutation in *FOXP2* [4], the first gene to be implicated in speech and language [5]. Neural and genetic properties of this disorder may enhance our understanding of the foundations of human speech [3, 6].

Based on the neural expression pattern of the *FOXP2*/*Foxp2* protein, Vargha-Khadem and colleagues [6] formulated a model whereby normal speech relies primarily on the modulation of activity in the ventral motor cortex via cortico-cortical pathways, as well as two major cortico-subcortical pathways, one fronto-striatal and the other fronto-cerebellar. Although abnormalities in the fronto-striatal circuit of affected KE members are well-documented [7–11], the significance of the abnormal fronto-cerebellar loops remains unexplored. The need for their detailed study is highlighted by the strikingly early and prominent expression of *Foxp2*/*FoxP2*/*FOXP2* in

rodent, avian and human cerebella, respectively, compared with other structures [12–19]. Moreover, the cerebellum shows massive computational power (the adult male human cerebellum contains 80% of brain neurons [20]) and an equally striking evolutionary expansion of its hemispheres [21], in concert with their cerebral association input/output areas [22, 23]. Importantly, recent evidence in mice [24] suggests that the cerebellum modulates striatal activity and cortico-striatal plasticity via a short-latency, disynaptic cerebello-striatal pathway. Likewise, the segregated, reciprocal basal ganglia-cerebellum connectivity found in non-human primates [25, 26] suggests an interplay between cortico-striatal and cortico-cerebellar circuits in motor sequence learning in the adult human brain [27, 28].

Further, neuroimaging evidence from the adult brain implicates cerebellar lobules HVI/HVIIa Crus I,¹ left inferior frontal gyrus, premotor and supplementary motor cortex in articulatory rehearsal during verbal working memory encoding [30–33] and increased speech complexity [34]. This is in line with recent findings associating the impaired phonological working memory of affected KE members with deficits in subvocal rehearsal of speech-based material [35]. Lobules HVI/HVIIa Crus I also show somatotopically organized responses for complex movements in healthy adults [36].

In view of the above, we used advanced methods to conduct spatially precise analyses of cerebellar MRIs [37] in order to identify structural and functional abnormalities in affected KE members. We predicted that HVI/HVIIa Crus I would show the largest cerebellar structural abnormality in affected KE members relative to both unaffected members and unrelated controls. We expected that these abnormalities would be bilateral, in accordance with our previous findings on early onset speech and language disorders, where unilateral abnormality offers greater opportunity for compensation in the developing brain [38, 39]. This pattern would also be consistent with the bilateral reduction in GM volume in the caudate nucleus, and the increase in the putamen [8], as well as the bilateral HVI/HVIIa Crus I activations for verbal working memory [40] and complex movements [36]. Furthermore, HVI/HVIIa Crus I were expected to show pronounced functional abnormalities (fMRI) during non-word repetition. Problems in this task provide a reliable marker of speech and language impairment, and performance is strongly predicted by oromotor praxis in neurotypical development [41]. We also expected that the asymmetry and/or volume of HVI/

HVIIa Crus I would correlate with accuracy in non-word repetition and non-verbal orofacial praxis, two key aspects of the behavioural phenotype of this mutation [42]. Finally, we examined the structural covariance of these lobules with the caudate nucleus in affected KE members, in light of the engagement of cerebellar-basal ganglia circuitry in finely timed motor control [24].

Materials and Methods

We used structural MRI datasets acquired from different subsets of affected KE members at three time points and reported previously (time-point 1: [7–9, 43]; time-point 2: [44]; time-point 3: [11]) and fMRI data for non-word repetition [11].

Participants

Demographic details of participants in each of the three time points are outlined in Table 1. All of the affected KE members who were available and eligible for brain imaging had been originally scanned at time point 1 ($n = 10$). At time points 2 (delay from time point 1: mean = 9.17; SD = 0.45 years) and 3 (delay from time point 1: mean = 11.50; SD = 0.58 years), subsets of those individuals (time point 2: $n = 6$; time-point 3: $n = 4$) were available for recruitment.

Data Acquisition

MRI (Time Point 1–3)

Details of structural MRI acquisition at each time point are reported in Table S1.

fMRI (Time Point 3)

Further details on this study can be found in [11]. Briefly, here, two runs of 60 volumes were collected for each participant at time point 3 (see Table 1), with five task/baseline blocks (one block = 6 volumes) per run. During the task period (non-word repetition), each non-word was presented via headphones and was immediately repeated aloud by the participant. During baseline, white noise bursts were presented.

Cerebellar Morphometry and Lobular Volumetry (Time Points 1–3)

We combined cerebellum-specific voxel-based morphometry (VBM) and lobular volumetry using SUIT (v. 3.1; <http://www.icn.ucl.ac.uk/motorcontrol/imaging/suit.htm>; [37]) in SPM12 (v. 6225; Wellcome Department of Cognitive Neurology, London, UK) running in Matlab 2015a (The MathWorks, Inc., Natick, MA, USA). Compared with

¹ We follow the nomenclature used in the ‘MRI Atlas of the Human Cerebellum’ [29]: cerebellar lobules are labelled ‘I-X’ from the anterior-superior border, through posterior-superior, posterior-inferior, to the anterior-inferior border. The nomenclature is based on that of Larsell and Jansen [21], where cerebellar hemispheres are distinguished from the vermis with the ‘H’ prefix. The atlas of Schmahmann and colleagues [29] uses this prefix to refer specifically to the hemispheres, and the adjective ‘vermal’ to refer to vermal compartments of a lobule. No prefix is used when referring to the entire lobule.

Table 1 Details of affected ('A'), unaffected ('U') KE members or unrelated controls ('C') scanned at three time points

Participants						
Time point	Groups	N	Age (years)			Sex (n females)
			Mean	Min	Max	
1	Affected (A1–A10)	10	29.30	9	77	5
	Unaffected (U1–U5)	5	15.20	9	21	2
	Controls (C1–C9)	9	33.67	21	77	5
2	Affected (A1–A6)	6	33.00	19	57	3
	Controls* (C10–C15)	6	34.21	20	63	3
	Unaffected (U1–U4, U6–U7)	6	26.02	21	29	3
3	Controls* (C16–C21)	6	27.16	23	31	3
	Affected (A1–A4)	4	32.00	22	53	2
	Controls* (C22–C25)	4	31.75	22	52	2

*Controls were individually matched for handedness, age (± 6 years), and sex with affected/unaffected members. Time point 1 = four affected and three unaffected members were 9–18 years of age. All others were adults. No overt focal abnormalities were detectable. Unrelated controls and unaffected members had no known history of speech-language, neurological, hearing or developmental impairment. All were native English speakers

normalization to the MNI whole-brain template, SUI provides stronger contrast for the cerebellum, improving fissure overlap among subjects by reducing spatial variance to 1/3.

Cerebellum-Specific VBM (Time Points 1–3)

T₁-weighted images were re-orientated so that the origin coordinates lay over the anterior commissure and segmented into grey matter (GM), white matter (WM) and CSF, using the unified segmentation procedure [45]. The cerebellum and brainstem were isolated and a mask was created per scan, which was manually corrected using MRICron [46] (<http://www.mccauslandcenter.sc.edu/mricro/mricron>) as non-cerebellar regions (e.g. transverse sinus, bone marrow) are occasionally misclassified as cerebellar GM [37]. Using SUI's DARTEL-algorithm, the cerebellum was deformed to fit the probability maps of cortical GM and WM to an atlas template. Nonlinear deformation was applied to GM segmentation maps, which were modulated to compensate for volume changes during normalization, by multiplying the intensity value in each voxel with Jacobian determinants. The amount of GM signal in normalized images was thus preserved, with VBM statistics reflecting GM volume differences [47, 48]. Images were smoothed with an isotropic Gaussian kernel of 4 mm full-width at half-maximum (FWHM), in line with previous cerebellar VBM studies [49, 50]. GM differences between groups were assessed by voxel-wise *t* test analyses. Whenever participants in the groups were not individually matched, sex and age were entered as between-subjects covariates (ANCOVA). Comparisons were conducted separately for each subset/time point. Given the small smoothing kernels employed for spatial precision in these analyses, we applied stringent corrections for multiple comparisons (voxel peak-

cluster-level familywise error (FWE)-correction: $p < .005$) and non-stationary smoothness [51] over an individual voxel threshold of $p < .001$.

Cerebellar Lobular Volumetry (Time Points 1–3)

The procedure involved cropping and isolating the cerebellum, SUI normalization, re-slicing the cerebellar atlas into subject space using the deformation parameters from normalization and calculating the number of voxels in each lobule in the re-sliced images. One of the authors (GPDA) corrected the cerebellar isolation masks and the re-sliced cerebellar atlas while blind to the participant's identity. This process resulted in volumetric measurements of cerebellar lobules (left, right I–IV, V; left, medial [vermal], or right hemispheric VI, VIIa Crus I, VIIa Crus II, VIIb, VIIIa, VIIIb, IX and X). For all comparisons, volumes were expressed both in cc and as a proportion of cerebellar cortical volume. As in VBM, ANCOVAs were used with age and sex as covariates. We predicted a main effect of group for Crus I volume, and a group \times lobule interaction. Comparisons were conducted separately for each time-point. Significance for two-tailed tests was set at $p < .05$, using Tukey's honestly significant difference (HSD) to correct for multiple comparisons. Violations of the sphericity assumption (tested by Mauchly's *W*) were followed by a Huynh-Feldt correction of degrees of freedom. Hemispheric asymmetry was calculated for Crus I using the formula (right – left/right + left hemisphere) [52].

Structure-Function Relationships (Time Point 1)

We examined the correlation (Pearson's *r*; SPSS, v. 22) of Crus I volume and asymmetry with the behavioural measures

reported to fully dissociate affected from unaffected members [42] and to correlate with the affected members' caudate volume (time point 1; [8]): (i) *Non-word repetition*: Participants heard and repeated 40 non-words [53], half of which contained consonant clusters ('complex' non-words). The dependent measure was the number of complex non-words accurately repeated; (ii) *Non-verbal orofacial praxis*: A rating scale was used to assess the performance of orofacial movements [42]. We predicted that the number of accurately repeated complex non-words and the orofacial movement ratings would correlate with Crus I volumetric measures from the same time-point.

fMRI Analysis (Time Point 3)

After realignment, preprocessing of EPIs followed the same steps as in cerebellar VBM, apart from modulation. We compared task (non-word repetition) vs. baseline (listening to white noise bursts), using the fixed-effects analysis employed in [11], reporting regions active in the group as a whole (time point 3). We identified regions that were both activated in controls ($n = 4$; inclusive mask threshold for 'task > baseline: $p < .01$) and less/more active in affected members ($n = 4$). The same stringent FWE corrections were applied as those in our VBM analyses.

Structural Covariance of Vlla Crus I and Caudate Nucleus (Time Point 1)

In order to explore the structural covariance of the caudate nucleus with lobules that were structurally/functionally abnormal in affected KE family members, we first examined the correlation of the previously measured volumes of the caudate nuclei corrected for total intracranial volume (TICV) from time point 1 [8] with GM volume across the whole brain (VBM regression). The pre-processing pipeline was the same as that for cerebellar VBM, with the exception that GM

images were normalized to MNI space by generating a group-specific whole-brain template (DARTEL), and an 8-mm³ FWHM smoothing kernel was used. Age and sex were entered as covariates and total caudate volume as a main effect regressor. We expected to identify clusters in the caudate nuclei bilaterally, given that volumetry and VBM measure the same effects [54], but also in structures the volume of which would covary with the caudate nucleus, probably due to common experience-related plasticity or mutually trophic influences, driven by environmental and genetic factors [48]. We subsequently focused on bivariate correlations (Pearson's r) between TICV-corrected left/right/total caudate nucleus volumes and TICV-corrected left/right hemispheric/medial/total volumes of lobules that showed structural/functional abnormalities consistently across time-points.

Results

Groups did not differ in TICV, whole-brain, or cerebellar cortical GM volume (between-groups comparisons across time points: $p \geq .10$; Table 2).

Cerebellar Lobular Volumetry (Time Points 1–3)

Across time points, affected members showed smaller Crus I volume relative to unaffected members and unrelated controls (Fig. 1; Table 3; time point 1 = -18%; time point 2 = -21%; time point 3 = -21%), but did not differ consistently in any other lobule (Table S2). Results were replicated with (a) age and sex as between-subjects covariates (Table S3); (b) when left, right hemispheric and medial volumes were compared separately (Fig. S1); (c) when volume was expressed as percent cerebellar cortex (Table S3; Fig. S2). Unaffected KE members did not differ from unrelated controls in any lobule (time points 1 and 2).

Table 2 TICV, whole-brain GM and cerebellar cortical GM for affected, unaffected KE family members, and unrelated controls in each of the three time points; F and p values pertain to between-subjects ANOVAs

Time point	Group	TICV (cc)		Whole-brain GM (cc)		Cerebellar cortex GM (cc)	
		Mean (SD)	F (p)	Mean (SD)	F (p)	Mean (SD)	F (p)
1	Affected	1465.63 (116.49)	0.42 (0.66)	1043.30 (65.10)	1.13 (0.34)	122.62 (9.85)	2.22 (0.13)
	Unaffected	1531.15 (153.92)		1101.56 (129.95)		135.95 (13.19)	
	Controls	1504.50 (151.35)		1009.64 (135.60)		131.95 (15.31)	
2	Affected	1353.00 (84.52)	1.11 (0.35)	979.61 (67.72)	0.71 (0.51)	120.94 (11.34)	2.58 (0.10)
	Unaffected	1447.02 (157.93)		1046.18 (106.40)		134.40 (12.45)	
	Controls	1456.45 (156.60)		1032.54 (117.80)		140.90 (21.47)	
3	Affected	1479.96 (93.92)	2.64 (0.16)	1010.78 (27.92)	0.06 (0.81)	107.29 (7.76)	2.72 (0.15)
	Controls	1578.07 (75.77)		1024.14 (100.52)		119.28 (12.29)	

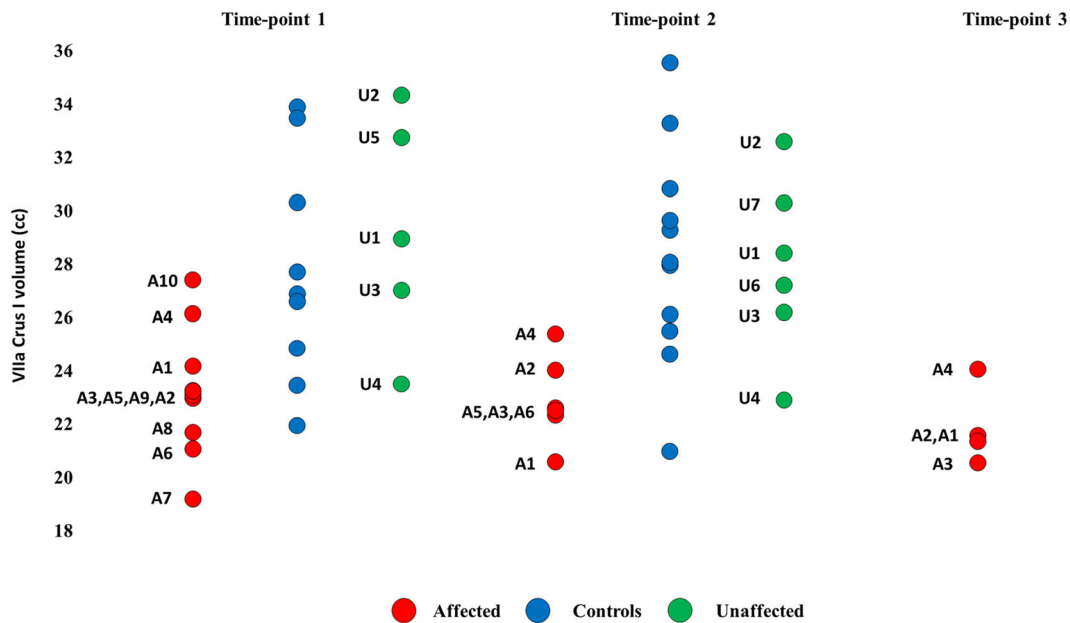


Fig. 1 Lobular volumetry for VIIa Crus I. Red = affected. Green = unaffected. blue = controls (unrelated). Volumes of VIIa Crus I are expressed in cc. A = affected. U = unaffected KE family members

Cerebellum-Specific VBM (Time Points 1–3)

The VBM analyses showed a number of regions with reduced GM volume in affected KE members relative to unrelated controls and unaffected KE members. These included medial IV–VI and hemispheric portions of VIIb–VIIIb. Nevertheless, the only discrepancy consistent across time points and comparison groups was the GM volume reduction in HVIIa Crus I

of affected members (Fig. 2; Tables S4–6; Fig. S3), shown to be bilateral in most comparisons.

Structure-Function Analysis (Tim Point 1)

The number of accurately repeated complex non-words and the orofacial praxis ratings correlated negatively with VIIa Crus I volumetric measures (Fig. 3), but not with any

Table 3 All post hoc tests were HSD-corrected for multiple comparisons; ‘affected’ = affected KE members; ‘unaffected’ = unaffected KE members; ‘controls’ = unrelated controls; the dependent measure is volume expressed in cc

Time points	Group comparisons	
1	Between-subjects ANOVAs (Group: affected, unaffected, controls)	Group: VIIa Crus I: $F_{(2,21)} = 6.18, p = .008$ (Affected vs. controls: $p = .033$; affected vs. unaffected: $p = .014$)
	Mixed-effects ANOVA (Group: affected, unaffected, controls; lobule: I–X)	Group \times lobule: $F_{(4,71, 49,41)} = 4.03, p = .004$
2	Pairwise t tests (affected vs. controls*)	VIIa Crus I: $t_{(5)} = -3.89, p = .012$
	Repeated measures ANOVA (Group: affected, controls*; lobule: I–X)	Group \times lobule: $F_{(1,80, 9,00)} = 9.65, p = .007$
	Between-subjects ANOVA (Group: affected, unaffected, controls)	Group: VIIa Crus I: $F_{(2,15)} = 7.66, p = .005$ (Affected vs. controls: $p = .008$; affected vs. unaffected: $p = .014$)
3	Mixed-effects ANOVA (Group: affected, unaffected, controls; lobule: I–X)	Group \times lobule: $F_{(4,95,37,11)} = 4.00, p = .005$
	Paired samples t test (affected vs. controls*)	VIIa Crus I: $t_{(3)} = -5.12, p = .014$
	Repeated-measures ANOVA (Group: affected, controls*; lobule: I–X)	Group \times lobule: $F_{(5,76, 17,27)} = 14.73, p = .000007$

*Controls were individually matched for handedness, age (± 6 years), and sex with affected/unaffected members

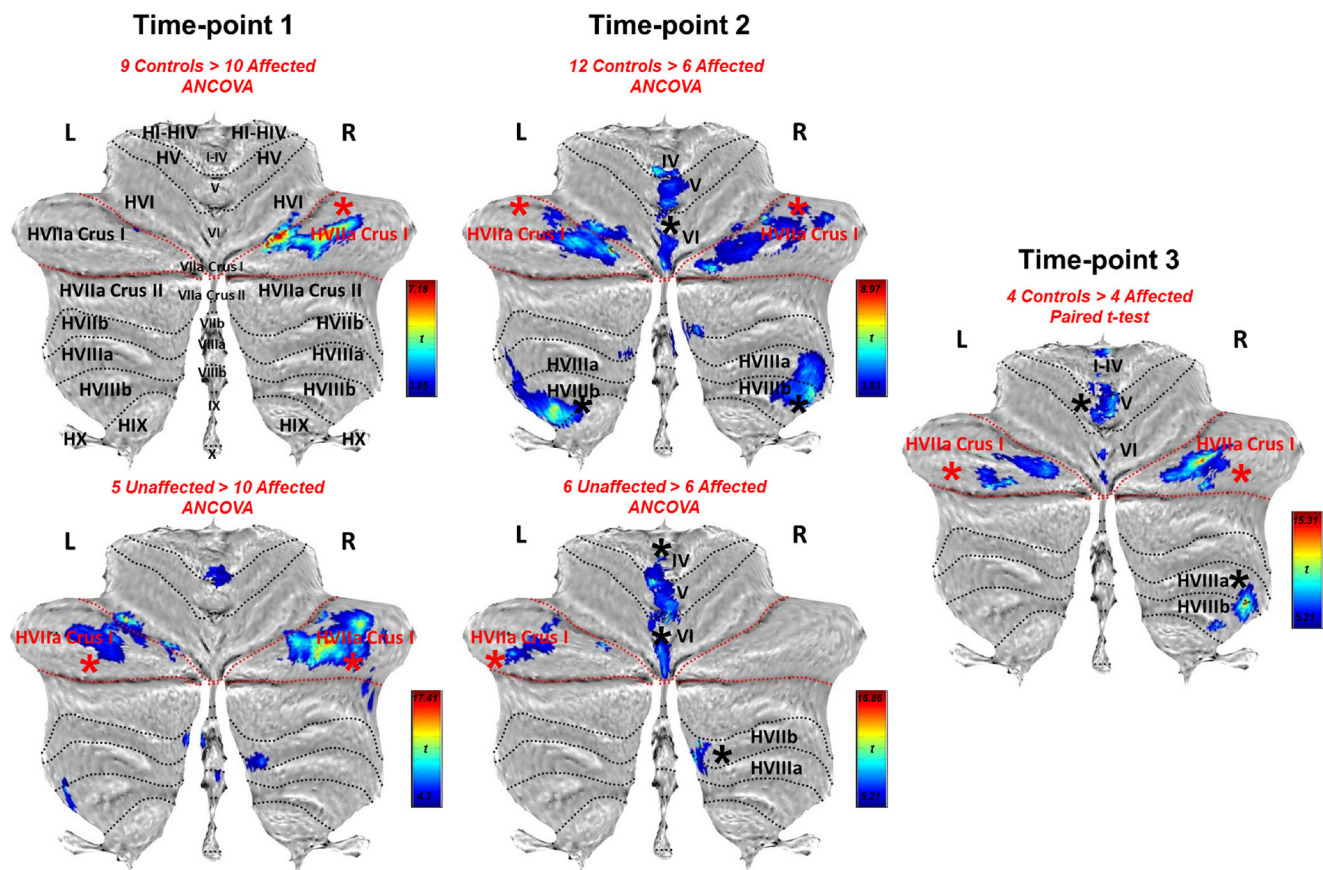


Fig. 2 VBM. Red lines = superior-posterior and horizontal fissures, delineating VIIa Crus I in flatmap [55]; black asterisk = clusters survive correction for non-stationary smoothness and FWE ($p < .005$) over voxel threshold of $p < .001$; red asterisk = significant clusters in HVIIa Crus I are found across time points and comparisons, unlike all other lobules

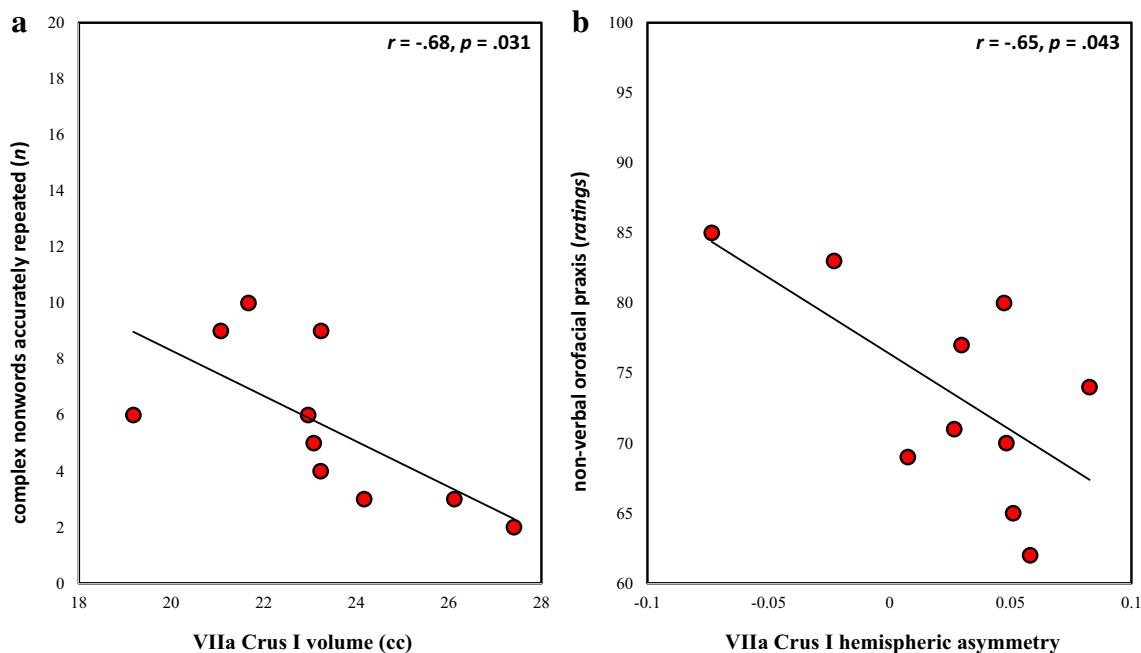


Fig. 3 Structure-function relationships. **a** Correlation of total VIIa Crus I volume with the number of accurately repeated complex non-words. Right HVIIa Crus I volume correlated with the same measure, expressed either in cc ($r = -.64, p = .048$) or in percent cerebellar cortex ($r = -.64, p = .047$); left HVIIa Crus I volume correlated at marginal

levels with the same measure when expressed in cc ($r = -.62, p = .054$). **b** Correlation of orofacial praxis ratings with Crus I hemispheric asymmetry; right HVIIa Crus I volume (cc) marginally correlated with the same measure ($r = -.60, p = .069$)

other lobular volumes (all ps , $p > .15$). The same negative correlations have already been reported for the right and total caudate nucleus volume [8]. Using a series of partial correlation analyses, we thus sought to examine whether right/total HVIIa Crus I volumes would correlate with these scores above and beyond right/total caudate nucleus volumes, and vice versa. As expected, no significant partial correlation was shown, given the strong positive volumetric correlations of these two structures in affected KE members (Table S7).

fMRI Analysis (Time Point 3)

There was reduced activity in HVI/HVIIa Crus I bilaterally in affected KE members relative to matched controls during non-word repetition compared with the noise-burst baseline (Fig. 4).

Structural Covariance of HVIIa Crus I and Caudate Nucleus (Time Point 1)

Crus I and caudate nuclei showed structural covariance in affected KE members. This was seen in whole-brain VBM regression, where total caudate volume expectedly correlated bilaterally with GM volume in the caudate nuclei (Fig. S4), but also with regions in the right HVIIa Crus I and the left supplementary motor area (SMA) (Fig. 5). The same

relationship was seen between the previously measured volumes of the caudate nuclei [8] and those of Crus I (Fig. 6).

Discussion

The speech and language deficits in half the members of the KE family are associated with a point mutation in *FOXP2*. Its neural and behavioural phenotype may shed light on the ontogenetic and phylogenetic foundations of articulate speech. The structural and functional abnormalities in the fronto-striatal circuitry of affected KE members have been well documented. In particular, the caudate volume reduction bilaterally represents a fundamental component of this neural phenotype that is associated with key aspects of the behavioural phenotype of this mutation. Nevertheless, very little has been known so far about the fronto-cerebellar circuits, despite the very early expression pattern of the *FOXP2*/*Foxp2* protein in the cerebellum across species.

In this study, we identified a pronounced volume reduction ($\approx 20\%$ relative to unaffected members and unrelated controls) bilaterally in cerebellar VIIa Crus I in affected KE family members at all three of the different time points of MRI data collection. Their right hemispheric and total cerebellar Crus I volume correlated with their impaired performance in complex non-word repetition and non-verbal orofacial praxis. These two test scores reflect the core of the behavioural phenotype of this mutation [42]. Consistent with these structure-function relationships, the same lobule also showed hypoactivation bilaterally in non-word repetition. Importantly, the right hemispheric Crus I volume of affected members positively correlated with that of their left caudate nucleus, showing the same negative correlation with non-word repetition accuracy as that observed for the right (and total) caudate nucleus [8].

Our findings may thus reflect the presence of abnormalities in a cerebellar-striatal loop comprising HVIIa Crus I and the caudate nucleus. This proposal is based on evidence for reciprocal cerebellar-striatal connectivity in non-human primates [25, 26] and its role in finely timed motor control and learning in rodents [24]. It is also in line with human brain imaging studies that demonstrate resting-state functional connectivity of Crus I with the caudate nuclei [56] and the interplay of cortico-striatal with cortico-cerebellar circuits in motor sequence learning (e.g. [27, 28]). This is further supported by recent evidence for GM reduction in the caudate nucleus in patients with cerebellar atrophy [57], as well as findings highlighting the involvement of cerebellar pathology in disorders of the basal ganglia [58–60].

There are at least two possible explanations of the abnormalities described here. Firstly, Crus I regions may support speech motor sequencing across the lifespan. Studies on neurotypical adults suggest that HVI/HVIIa Crus I support

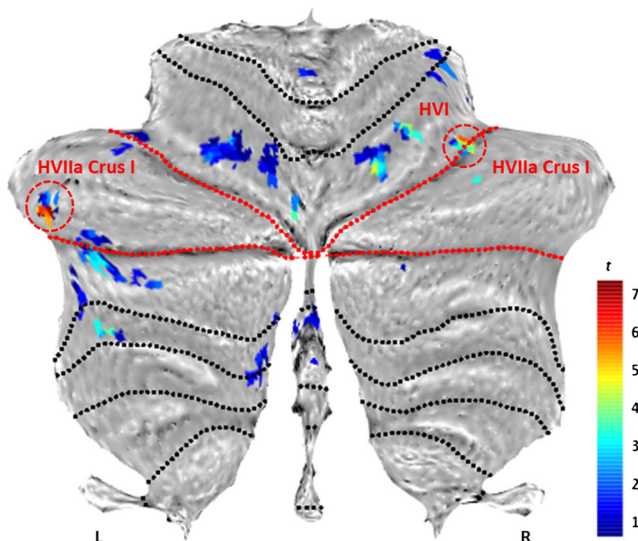
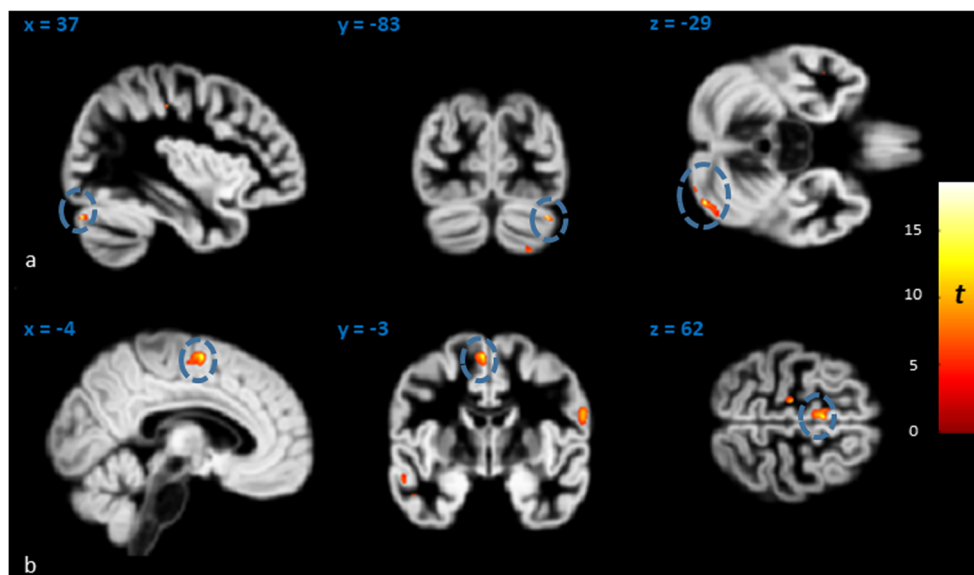


Fig. 4 Underactivations in affected members compared to matched controls for ‘non-word repetition > noise perception’. Red lines = superior posterior and horizontal fissures, delineating VIIa Crus I in the flatmap (Diedrichsen and Zotow [55]). Red circles = clusters surviving FWE correction ($p < .005$) at peak level over $p < .001$ (unc.): left HVIIa Crus I: $x = -46$, $y = -48$, $z = -37$ mm; $t = 6.77$, $z = 6.68$, $k_E = 4$ vox.; right HVI/HVIIa Crus I: $x = 34$, $y = -54$, $z = -31$ mm; $t = 5.94$, $z = 5.88$, $k_E = 3$ vox.). The left cluster survives a stringent inclusive threshold mask of $p < .001$. Results do not differ with a larger smoothing kernel (6-mm FWHM)

Fig. 5 Volumes of the caudate nuclei correlated with GM volume in **a** right HVIIa Crus I and **b** left SMA. Only these two clusters (blue circles; superimposed on whole-brain GM template in MNI space) survived correction for non-stationary smoothness and FWE at cluster level ($p < .005$) over an individual voxel threshold of $p < .001$



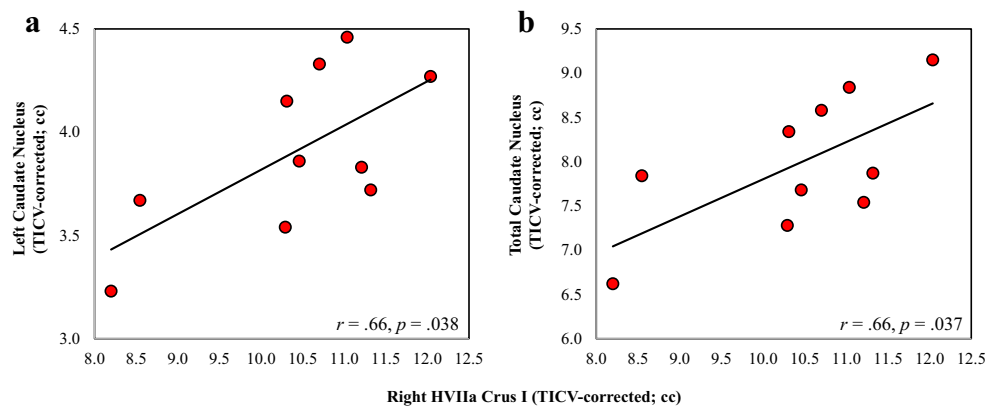
motor speech sequencing [61–63], and are somatotopically organized selectively for the production of complex motor sequences [36]. While cerebellar damage is associated with ataxic dysarthria [64], the diminished sequence length effects on speech reaction times noted in cases of ataxic dysarthria have been held to reflect impaired ‘motor programming’ [65]. Interestingly, a recent study has shown effects of non-invasive stimulation of the right HVIIa Crus I/II on phonological errors in speech production (addition, deletion, transposition of phonemes) in neurotypical adults [66]. Crossed cerebellar diaschisis-related phenomena may also play an important role in apraxias of speech [67–71]. Indeed, Broca’s area (44/45), which also shows structural and functional abnormalities in affected KE members [8–11], is embedded in common functional networks with the adult HVI/HVIIa Crus I [72]. This circuitry is activated during verbal working memory encoding, motor rehearsal [30, 32–34], and modulated by difficulty in overt non-word reading [61].

A second explanation is that Crus I regions are selectively important in the pre-automatic stage of motor learning in speech acquisition. Evidence that apraxia of speech occurs

as a cerebellar syndrome is quite limited [73]. There is, however, strong support for a cerebellar role in the acquisition of complex motor sequences [74–76]. With extended practice, cerebellar cortical activation decreases, paralleled by increases in cortico-striatal circuits [27], with regions close to SMA ultimately representing the automatized sequence [77]. Characteristically, the monkey pre-SMA, which, unlike SMA, is reciprocally connected with Crus I/II [78], is engaged in early motor sequence learning [79]. Similarly, pre-automatic processing of motor sequences is associated with activity in prefrontal cortex and HVI/HVIIa Crus I [80]. Regions in the caudate nucleus and Crus I are embedded within the ‘fronto-parietal control network’ [72, 81], which may be engaged during initial motor sequence learning (e.g. [82]). This dovetails with proposals that cerebellar integrity is of greater importance in earlier developmental stages [83]. Similar proposals have been made for the striatum in speech acquisition [84, 85].

Further research is required to assess these explanations. This would include larger group sizes to examine the speech-related functional abnormalities observed in Crus I

Fig. 6 Correlation of right HVIIa Crus I volumes of affected KE family members with their **a** left caudate and **b** total caudate nucleus volumes. Total VIIa Crus I volume correlated at marginal levels with total caudate nucleus volume ($r = .61, p = .060$). All volumes are TICV-corrected (corrected for total intracranial volume in cc), in order to allow for the correlation of Crus I volumes calculated here with those of the caudate nuclei [8]



for the affected KE members, given the small sample sizes analysed here. T_1 - and T_2 -weighted MRI should also be conducted at higher field strength, in order to examine structural and functional abnormalities in the dentate nucleus, to which Purkinje cells of Crus I project. Moreover, our findings do not contradict the VIIb and VIIIb volume reductions in affected KE members reported earlier [8, 9], as some contrasts here disclosed reductions in medial IV–VI and hemispheric VIIb–VIIIb. The former are the loci for the somatotopic representation of the orofacial musculature [86]; the latter may be associated with the involvement of lobule VIII in auditory [87] and somatosensory feedback processing [88]. Finally, considering the inverse correlations of non-word repetition accuracy with both Crus I and right caudate volumes, it is likely that neurodevelopmental compensatory mechanisms, functional reorganization for caudate/Crus I reduction (see discussion in [8]), and additional disruptions in synaptic pruning could be involved.

Conclusion

Consistent with the early, homologous expression pattern of *FOXP2/Foxp2* in the human/rodent cerebellar cortical Purkinje cells, the neurodevelopmental abnormalities that we identify in lobule HVIIa Crus I of the affected members of the KE family may compromise the capacity of cerebellar-striatal circuitry to execute complex oromotor sequences. Our findings thus point towards abnormality in a circuit linking cerebellar lobule HVIIa Crus I with the caudate nucleus. This loop may be a fundamental component of the neural apparatus that enables the finely timed coordination of complex oromotor sequences needed for human speech. Research on the neurobiology of speech and language acquisition and processing needs to examine the complex interplay between cortico-striatal and cortico-cerebellar circuits, rather than their contributions in isolation from each other.

Acknowledgments The authors would like to thank the members of the KE family and all the other participants for their continued cooperation. The views expressed are those of the authors and not necessarily those of the NHS, the NIHR or the Department of Health.

Funding Information This study was funded by the Medical Research Council Grant G0300117/65439; Intramural Research Program of the National Institute of Mental Health, National Institutes of Health; Research and Development funding from the NHS Executive and supported by the National Institute for Health Research Biomedical Research Centre at Great Ormond Street Hospital for Children NHS Foundation Trust and University College London

Compliance with Ethical Standards

Conflict of Interest The authors declare that they have no competing interests.

Ethical Approval All procedures performed were in accordance with the ethical standards of the Ethics Committee of the Great Ormond Street Hospital for Children NHS Trust, the Great Ormond Street Institute of Child Health, and with the 1964 Helsinki declaration and its later amendments or comparable ethical standards. Informed consent was obtained from all individual participants included in the study.

Open Access This article is distributed under the terms of the Creative Commons Attribution 4.0 International License (<http://creativecommons.org/licenses/by/4.0/>), which permits unrestricted use, distribution, and reproduction in any medium, provided you give appropriate credit to the original author(s) and the source, provide a link to the Creative Commons license, and indicate if changes were made.

References

- Hurst JA, Baraitser M, Auger E, Graham F, Norell S. An extended family with a dominantly inherited speech disorder. *Dev Med Child Neurol.* 1990;32:352–5.
- Vargha-Khadem F, Passingham RE. Speech and language defects. *Nature.* 1990;346:226.
- Vargha-Khadem F, Watkins K, Alcock K, Fletcher P, Passingham R. Praxic and nonverbal cognitive deficits in a large family with a genetically transmitted speech and language disorder. *Proc Natl Acad Sci U S A.* 1995;92:930–3.
- Lai CSL, Fisher SE, Hurst JA, Vargha-Khadem F, Monaco AP. A forkhead-domain gene is mutated in a severe speech and language disorder. vol. 413. London: Nature Nature Publishing Group; 2001. p. 519–23.
- Konopka G, Roberts TF. Insights into the neural and genetic basis of vocal communication. *Cell.* 2016;164:1269–76.
- Vargha-Khadem F, Gadian DG, Copp A, Mishkin M. FOXP2 and the neuroanatomy of speech and language. *Nat Rev Neurosci.* 2005;6:131–8.
- Vargha-Khadem F, Watkins KE, Price CJ, Ashburner J, Alcock KJ, Connelly A, et al. Neural basis of an inherited speech and language disorder. *Proc Natl Acad Sci U S A.* 1998;95:12695–700.
- Watkins KE, Vargha-Khadem F, Ashburner J, Passingham RE, Connelly A, Friston KJ, et al. MRI analysis of an inherited speech and language disorder: structural brain abnormalities. *Brain.* 2002;125:465–78.
- Belton E, Salmond CH, Watkins KE, Vargha-Khadem F, Gadian DG. Bilateral brain abnormalities associated with dominantly inherited verbal and orofacial dyspraxia. *Hum Brain Mapp.* 2003;18:194–200.
- Liégeois F, Baldeweg T, Connelly A, Gadian DG, Mishkin M, Vargha-Khadem F. Language fMRI abnormalities associated with FOXP2 gene mutation. *Nat Neurosci.* 2003;6:1230–7.
- Liégeois F, Morgan AT, Connelly A, Vargha-Khadem F. Endophenotypes of FOXP2: dysfunction within the human articulatory network. *Eur J Paediatr Neurol.* 2011;15:283–8.
- Lai CSL, Gerrelli D, Monaco AP, Fisher SE, Copp AJ. FOXP2 expression during brain development coincides with adult sites of pathology in a severe speech and language disorder. *Brain.* 2003;126:2455–62.
- Ferland RJ, Cherry TJ, Preware PO, Morrisey EE, Walsh CA. Characterization of *Foxp2* and *Foxp1* mRNA and protein in the developing and mature brain. *J Comp Neurol.* 2003;460:266–79.
- Shu W, Cho JY, Jiang Y, Zhang M, Weisz D, Elder GA, et al. Altered ultrasonic vocalization in mice with a disruption in the *Foxp2* gene. *Proc Natl Acad Sci U S A.* 2005;102:9643–8.
- Fujita E, Tanabe Y, Shiota A, Ueda M, Suwa K, Momoi MY, et al. Ultrasonic vocalization impairment of *Foxp2* (R552H) knockin

- mice related to speech-language disorder and abnormality of Purkinje cells. *Proc Natl Acad Sci U S A*. 2008;105:3117–22.
16. Fujita E, Tanabe Y, Momoi MY, Momoi T. Cntnap2 expression in the cerebellum of Foxp2(R552H) mice, with a mutation related to speech-language disorder. *Neurosci Lett*. 2012;506:277–80.
 17. Takahashi K, Liu FC, Hirokawa K, Takahashi H. Expression of Foxp2, a gene involved in speech and language, in the developing and adult striatum. *J Neurosci Res*. 2003;73:61–72.
 18. Campbell AJ, Lyne L, Brown PJ, Launchbury RJ, Bignone P, Chi J, et al. Aberrant expression of the neuronal transcription factor FOXP2 in neoplastic plasma cells. *Br J Haematol*. 2010;149:221–30.
 19. Teramitsu I, Kudo LC, London SE, Geschwind DH, White SA. Parallel FoxP1 and FoxP2 expression in songbird and human brain predicts functional interaction. *J Neurosci*. 2004;24:3152–63.
 20. Azevedo FAC, Carvalho LRB, Grinberg LT, Farfel JM, Ferretti REL, Leite REP, et al. Equal numbers of neuronal and nonneuronal cells make the human brain an isometrically scaled-up primate brain. *J Comp Neurol*. 2009;513:532–41.
 21. Larsell O, Jansen J. The comparative anatomy and histology of the cerebellum. Minneapolis: The University of Minnesota Press; 1967.
 22. Leiner HC, Leiner AL, Dow RS. Does the cerebellum contribute to mental skills? *Behav Neurosci*. 1986;100:443–54.
 23. Whiting B, Barton R. The evolution of the cortico-cerebellar complex in primates: anatomical connections predict patterns of correlated evolution. *J Hum Evol*. 2003;44:3–10.
 24. Chen CH, Fremont R, Arteaga-Bracho EE, Khodakhah K. Short latency cerebellar modulation of the basal ganglia. *Nat Neurosci*. 2014;17:1767–75.
 25. Bostan AC, Dum RP, Strick PL. The basal ganglia communicate with the cerebellum. *Proc Natl Acad Sci U S A*. 2010;107:8452–6.
 26. Hoshi E, Tremblay L, Féger J, Carras PL, Strick PL. The cerebellum communicates with the basal ganglia. *Nat Neurosci*. 2005;8:1491–3.
 27. Doyon J, Song AW, Kami A, Lalonde F, Adams MM, Ungerleider LG. Experience-dependent changes in cerebellar contributions to motor sequence learning. *Proc Natl Acad Sci U S A*. 2002;99:1017–22.
 28. Tzvi E, Stoldt A, Witt K, Krämer UM. Striatal-cerebellar networks mediate consolidation in a motor sequence learning task: an fMRI study using dynamic causal modelling. *NeuroImage*. 2015;122:52–64.
 29. Schmahmann JD, Doyon J, Toga AW, Petrides M, Evans A. MRI atlas of the human cerebellum. San Diego: Academic Press; 2000.
 30. Desmond JE, Gabrieli JD, Wagner AD, Ginier BL, Glover GH. Lobular patterns of cerebellar activation in verbal working-memory and finger-tapping tasks as revealed by functional MRI. *J Neurosci*. 1997;17:9675–85.
 31. Chein JM, Fiez JA. Dissociation of verbal working memory system components using a delayed serial recall task. *Cereb Cortex*. 2001;11:1003–14.
 32. Chen SHA, Desmond JE. Cerebrocerebellar networks during articulatory rehearsal and verbal working memory tasks. *NeuroImage*. 2005;24:332–8.
 33. Chen SHA, Desmond JE. Temporal dynamics of cerebro-cerebellar network recruitment during a cognitive task. *Neuropsychologia*. 2005;43:1227–37.
 34. Marvel CL, Desmond JE. The contributions of cerebro-cerebellar circuitry to executive verbal working memory. *Cortex*. 2010;46:880–95.
 35. Schulze K, Vargha-Khadem F, Mishkin M. Phonological working memory and FOXP2. *Neuropsychol Pergamon*. 2018;108:147–52.
 36. Schlerf JE, Verstynen TD, Ivry RB, Spencer RMC. Evidence of a novel somatopic map in the human neocerebellum during complex actions. *J Neurophysiol*. 2010;103:3330–6.
 37. Diedrichsen J. A spatially unbiased atlas template of the human cerebellum. *NeuroImage*. 2006;33:127–38.
 38. Vargha-Khadem F, Mishkin M. Speech and language outcome after hemispherectomy in childhood. In: Tuxhorn I, Holthausen H, Boenigk HE, editors. *Paediatr epilepsy Syndr their Surg treat*. Montrouge: John Libbey & Co. Ltd. Medical Books; 1997. p. 774–84.
 39. Vargha-Khadem F, Carr LJ, Isaacs E, Brett E, Adams C, Mishkin M. Onset of speech after left hemispherectomy in a nine-year-old boy. *Brain*. 1997;120:159–82.
 40. Stoodley CJ, Valera EM, Schmahmann JD. Functional topography of the cerebellum for motor and cognitive tasks: an fMRI study. *NeuroImage*. 2012;59:1560–70.
 41. Krishnan S, Alcock KJ, Carey D, Bergström L, Karmiloff-Smith A, Dick F. Fractionating nonword repetition: The contributions of short-term memory and oromotor praxis are different. *PLoS One*. *Public Libr Sci*; 2017;12:e0178356.
 42. Watkins KE, Dronkers NF, Vargha-Khadem F. Behavioural analysis of an inherited speech and language disorder: comparison with acquired aphasia. *Brain*. 2002;125:452–64.
 43. Watkins KE, Gadian DG, Vargha-Khadem F. Functional and structural brain abnormalities associated with a genetic disorder of speech and language. *Am J Hum Genet*. 1999;65:1215–21.
 44. Belton E. The neural correlates of developmental speech and language disorders: a neuropsychological and neuroimaging investigation. University College London: Institute of Child Health; 2004.
 45. Ashburner J, Friston KJ. Unified segmentation. *NeuroImage*. 2005;26:839–51.
 46. Rorden C, Karnath H-OO, Bonilha L. Improving lesion-symptom mapping. *J Cogn Neurosci*. 2007;19:1081–8.
 47. Good CD, Johnsrude IS, Ashburner J, Henson RN, Friston KJ, Frackowiak RS. A voxel-based morphometric study of ageing in 465 normal adult human brains. *NeuroImage*. 2001;14:21–36.
 48. Mechelli A, Price CJ, Friston KJ, Ashburner J. Voxel-based morphometry of the human brain: methods and applications. *Curr Med Imaging Rev*. 2005;1:105–13.
 49. D'Agata F, Caroppo P, Baudino B, Caglio M, Croce M, Bergui M, et al. The recognition of facial emotions in spinocerebellar ataxia patients. *Cerebellum*. 2011;10:600–10.
 50. Peterburs J, Thürling M, Rustemeier M, Göricke S, Suchan B, Timmann D, et al. A cerebellar role in performance monitoring—evidence from EEG and voxel-based morphometry in patients with cerebellar degenerative disease. *Neuropsychologia*. 2015;68:139–47.
 51. Hayasaka S, Phan KLL, Liberzon I, Worsley KJ, Nichols TE. Nonstationary cluster-size inference with random field and permutation methods. *NeuroImage*. 2004;22:676–87.
 52. Snyder PJ, Bilder RM, Wu H, Bogerts B, Lieberman JA. Cerebellar volume asymmetries are related to handedness: a quantitative MRI study. *Neuropsychologia*. 1995;33:407–19.
 53. Gathercole SE, Baddeley AD. Evaluation of the role of phonological STM in the development of vocabulary in children: a longitudinal study. *J Mem Lang*. 1989;28:200–13.
 54. Focke NK, Trost S, Paulus W, Falkai P, Gruber O. Do manual and voxel-based morphometry measure the same? A proof of concept study. *Front Psychiatry Frontiers*. 2014;5:39.
 55. Diedrichsen J, Zotow E. Surface-based display of volume-averaged cerebellar imaging data. *PLoS One*. 2015;10:e0133402.
 56. Sang L, Qin W, Liu Y, Han W, Zhang Y, Jiang T, et al. Resting-state functional connectivity of the vermal and hemispheric subregions of the cerebellum with both the cerebral cortical networks and sub-cortical structures. *NeuroImage*. 2012;61:1213–25.
 57. Dayan M, Olivito G, Molinari M, Cercignani M, Bozzali M, Leggio M. Impact of cerebellar atrophy on cortical gray matter and cerebellar peduncles as assessed by voxel-based morphometry and high

- angular resolution diffusion imaging. *Funct Neurol*. 2016;31:239–48.
58. Wu T, Hallett M. The cerebellum in Parkinson's disease. *Brain*. 2013;136:696–709.
 59. Dirkx MF, den Ouden HEM, Aarts E, Timmer MHM, Bloem BR, Toni I, et al. Dopamine controls Parkinson's tremor by inhibiting the cerebellar thalamus. *Brain*. Oxford University Press; 2017;83:aww331.
 60. O'Callaghan C, Homberger M, Balsters JH, Halliday GM, Lewis SJG, Shine JM. Cerebellar atrophy in Parkinson's disease and its implication for network connectivity. *Brain*. 2016;139:845–55.
 61. Peeva MG, Guenther FH, Tourville JA, Nieto-Castanon A, Anton J-LL, Nazarian B, et al. Distinct representations of phonemes, syllables, and supra-syllabic sequences in the speech production network. *Neuroimage*. Elsevier Inc.; 2010;50:626–38.
 62. Fulbright RK, Jenner AR, Mencl WE, Pugh KR, Shaywitz BA, Shaywitz SE, et al. The cerebellum's role in reading: a functional MR imaging study. *Am J Neuroradiol*. 1999;20:1925–30.
 63. Bohland JW, Guenther FH. An fMRI investigation of syllable sequence production. *NeuroImage*. 2006;32:821–41.
 64. Morgan AT, Liégeois F, Liederkerke C, Vogel AP, Hayward R, Harkness W, et al. Role of cerebellum in fine speech control in childhood: persistent dysarthria after surgical treatment for posterior fossa tumour. *Brain Lang*. 2011;117:69–76.
 65. Spencer KA, Rogers MA. Speech motor programming in hypokinetic and ataxic dysarthria. *Brain Lang*. 2005;94:347–66.
 66. Runnqvist E, Bonnard M, Gauvin HS, Attarian S, Trébuchon A, Hartsuiker RJ, et al. Internal modeling of upcoming speech: a causal role of the right posterior cerebellum in non-motor aspects of language production. *Cortex*. 2016;81:203–14.
 67. Mariën P, Engelborghs S, Fabbro F, De Deyn PP. The lateralized linguistic cerebellum: a review and a new hypothesis. *Brain Lang*. 2001;79:580–600.
 68. Mariën P, Verhoeven J, Engelborghs S, Rooker S, Pickut BA, De Deyn PP. A role for the cerebellum in motor speech planning: evidence from foreign accent syndrome. *Clin Neurol Neurosurg*. 2006;108:518–22.
 69. Mariën P, Verhoeven J. Cerebellar involvement in motor speech planning: some further evidence from foreign accent syndrome. *Folia Phoniatri Logop*. 2007;59:210–7.
 70. Cohen DA, Kurowski K, Steven MS, Blumstein SE, Pascual-Leone A. Paradoxical facilitation: the resolution of foreign accent syndrome after cerebellar stroke. *Neurology*. 2009;73:566–7.
 71. Keulen S, Mariën P, Wackenier P, Jonkers R, Bastiaanse R, Verhoeven J. Developmental foreign accent syndrome: report of a new case. *Front Hum Neurosci Front*. 2016;10:65.
 72. Buckner RL, Krienen FM, Castellanos A, Diaz JC, Yeo BTT. The organization of the human cerebellum estimated by intrinsic functional connectivity. *J Neurophysiol*. 2011;106:2322–45.
 73. Ziegler W. The phonetic cerebellum: cerebellar involvement in speech sound production. In: Mariën P, Manto M, editors. *Linguist Cerebellum*. Amsterdam: Elsevier; 2016. p. 1–32.
 74. Carrera E, Tononi G, Abe O, Okubo T, Hayashi N, Saito N, et al. Diaschisis: past, present, future. *Brain*. 2014;137:2408–22.
 75. Laforce R, Doyon J. Distinct contribution of the striatum and cerebellum to motor learning. *Brain Cogn*. 2001;45:189–211.
 76. Lang CE, Bastian AJ. Cerebellar damage impairs automaticity of a recently practiced movement. *J Neurophysiol*. 2002;87:1336–47.
 77. Tanji J, Shima K. Supplementary motor cortex in organization of movement. *Eur Neurol*. 1996;36:13–9.
 78. Kelly RM, Strick PL. Cerebellar loops with motor cortex and prefrontal cortex of a nonhuman primate. *J Neurosci*. 2003;23:8432–44.
 79. Nakamura K, Sakai K, Hikosaka O. Neuronal activity in medial frontal cortex during learning of sequential procedures. *J Neurophysiol*. 1998;80:2671–87.
 80. Sakai K, Hikosaka O, Nakamura K. Emergence of rhythm during motor learning. *Trends Cogn Sci*. 2004;8:547–53.
 81. Choi EY, Yeo BTT, Buckner RL. The organization of the human striatum estimated by intrinsic functional connectivity. *J Neurophysiol*. 2012;108:2242–63.
 82. Jenkins IH, Brooks DJ, Nixon PD, Frackowiak RS, Passingham RE. Motor sequence learning: a study with positron emission tomography. *J Neurosci*. 1994;14:3775–90.
 83. Wang SSH, Kloth AD, Badura A. The cerebellum, sensitive periods, and autism. *Neuron*. 2014;83:518–32.
 84. Ullman MT. Is Broca's area part of a basal ganglia thalamocortical circuit? *Cortex*. 2006;42:480–5.
 85. Ackermann H, Hage SR, Ziegler W. Brain mechanisms of acoustic communication in humans and nonhuman primates: an evolutionary perspective. *Behav Brain Sci*. 2014;37:529–46.
 86. Schoch B, Dimitrova A, Gizewski ER, Timmann D. Functional localization in the human cerebellum based on voxelwise statistical analysis: a study of 90 patients. *NeuroImage*. 2006;30:36–51.
 87. Tourville JA, Reilly KJ, Guenther FH. Neural mechanisms underlying auditory feedback control of speech. *NeuroImage*. 2008;39:1429–43.
 88. Gollinopoulos E, Tourville JA, Bohland JW, Ghosh SS, Nieto-Castanon A, Guenther FH. fMRI investigation of unexpected somatosensory feedback perturbation during speech. *NeuroImage*. 2011;55:1324–38.